Bull. Korean Chem. Soc. **2014**, Vol. 35, No. 10 3077
http://dx.doi.org/10.5012/bkcs.2014.35.10.3077

Notes

Thermal Modulation of Photoluminescence from Single-Layer MoS_2

Yejin Ryu,[a] Min Kyu Park,[a] and Sunmin Ryu*

*Department of Applied Chemistry, Kyung Hee University, Yongin, Gyeonggi 446-701, Korea. *E-mail: sunryu@khu.ac.kr*

Received April 18, 2014, Accepted June 3, 2014

Key Words : MoS_2, Photoluminescence, Charge transfer doping, Hydrogen, Raman spectroscopy

The first mechanical exfoliation[1] of graphene from graphite in 2004 lead to emergence of various related two-dimensional crystals that can be practically defined as one or few-atom-thick crystalline materials. Graphene,[2] MoS_2[3] and h-BN[4] representing respectively the conducting, semiconducting and insulating two-dimensional material groups have great potentials in the applications such as nano-electronics, transparent conductive electrodes, barrier materials, multifunctional composites, *etc.* Their unique electronic structures mainly invoked for their promising applications are distinct from those of their bulk counterparts and originate from the electronic confinement within a few atoms along the z-axis or equivalently lack of interlayer interaction.[5]

Unlike the conducting graphene, single-layer (1L) MoS_2 with a direct bandgap of 1.8 eV exhibits strong photoluminescence (PL)[3,6] and has revealed unique optical properties such as thickness-dependent PL quantum yield,[3,6] valley polarization,[7] exciton-trion equilibrium,[8] *etc*. 1L MoS_2 is in fact a trilayer entity consisting of one hexagonal Mo atom layer sandwiched by two S atom layers with trigonal prismatic coordination by 6 S atoms per Mo atom.[9]

Bulk 2H-MoS_2 with an indirect bandgap of 1.2 eV,[3] the most common polytype found in the natural molybdenite, can be formed by repeating a Bernal-like van der Waals stack of two 1L MoS_2 layers with lattice constants of a = 0.316 nm and c = 1.229 nm.[10] As decreasing the number of layers or thickness, the electronic structure of MoS_2 undergoes a change from the indirect bandgap to the direct bandgap[3,6] and its lattice vibration also exhibits unique and anomalous progressions for E^1_{2g} and A_{1g} modes,[11] suggesting that its various other material properties should also be affected.

Since PL serving as a sensitive probe for the electronic structure is strong for 1L unlike the bulk MoS_2, PL spectroscopy has recently been a key diagnostic method for the two-dimensional MoS_2 along with Raman spectroscopy.[3,6] In particular, it was shown that the PL intensity can be modulated by electrostatic control of excess charge carriers in 1L MoS_2.[8,12] This fact in turn suggests that the charge density can be determined by the PL spectroscopy, which will allow us to explore otherwise overlooked subtle interfacial charge transfer reactions occurring between the two-dimensional materials and the environment.

In this study, we report that the PL intensity can be thermally modulated by annealing 1L MoS_2 in a vacuum or H_2 gas. The increase in the hole density and PL intensity induced by annealing in a vacuum was attributed to O_2-induced charge transfer occurring at the MoS_2-silica interface. Thermal treatment in the H_2 atmosphere induced decrease in the PL intensity, thus rise in excess electron density. This study demonstrates the thermal control of the photophysical properties of 1L MoS_2 and the diagnostic utility of the PL spectroscopy in the interfacial sciences.

Figure 1(a) shows the optical micrograph of thin MoS_2 samples prepared by the micromechanical exfoliation. The typical size of thin flakes was several microns across.

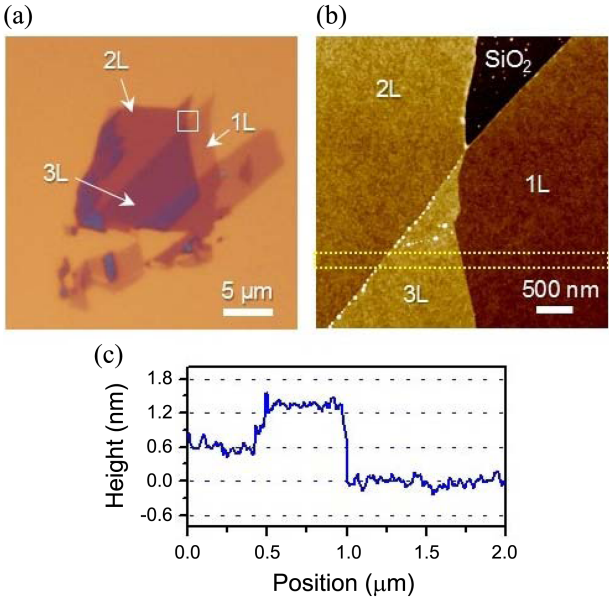

Figure 1. Topographic detail of single- and few-layer MoS_2. (a) Optical micrograph. The number (n) of layers is represented by "nL". (b) Non-contact AFM height image obtained from the region in the white square of (a). (c) The height profile averaged along the yellow dotted rectangle in (b), which shows ~0.6-nm-high steps between adjacent layers.

[a]These authors contributed equally to this work.

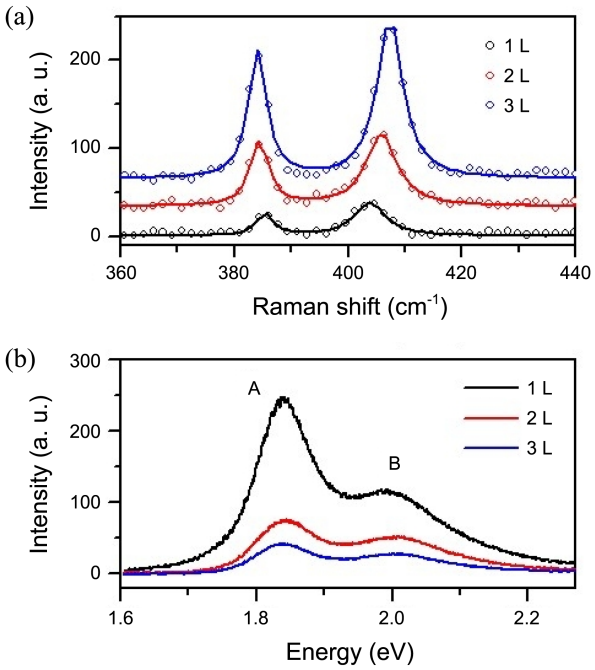

Figure 2. (a) Raman spectra of pristine 1L, 2L and 3L MoS_2. The lower and higher frequency peaks originate from E^1_{2g} and A_{1g}, respectively. The Raman spectra were offset vertically for clarity. (b) PL spectra of pristine 1L, 2L and 3L MoS_2. The A and B peaks denote the A and B excitons, respectively. Each of the PL spectra was normalized with respect to its Raman peak intensity.

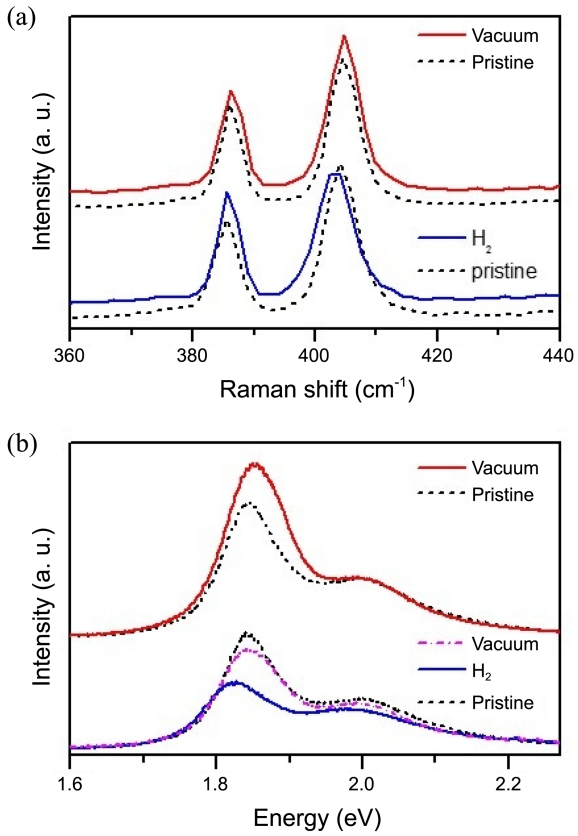

Figure 3. Effects of thermal treatments on Raman and PL spectra of 1L MoS_2. (a) Raman spectra before and after annealing in a vacuum (400 °C) and H_2 gas (500 °C). The Raman spectra were offset vertically for clarity. (b) PL spectra before and after annealing in a vacuum (400 °C) and H_2 gas (500 °C). The spectrum labeled as "vacuum" in magenta dash-dotted line was obtained after vacuum-annealing (2 h at 400 °C) following H_2-annealing at 500 °C.

Thicker layers appear darker due to the increasing optical density,[13] which can be useful in locating appropriate flakes on the SiO_2/Si substrates. The AFM image in Figure 1(b) shows that the basal planes of the flakes are highly flat and that there is discrete height difference between layers of different thickness. The height profile across the 1L-3L-2L area in Figure 1(c) reveals that the average thickness of one layer is *ca.* 0.67 ± 0.05 nm, which agrees well with the interplanar distance of bulk 2H-MoS_2 crystals.[14]

The number of layers and crystalline quality of the prepared samples were further investigated using Raman and PL spectroscopy. Raman spectroscopy, in particular, has been widely used to determine various properties of graphene such as thickness, defects, charge density, mechanical strain, *etc*.[15,16] Recently, Lee *et al.* demonstrated a similar diagnostic usage of Raman spectroscopy in determining the thickness of MoS_2 samples.[11] It is known that bulk 2H-MoS_2 has 4 Raman active normal modes in the long wavelength limit.[9] Since E_{1g} (~287 cm^{-1}) and E^2_{2g} (~34 cm^{-1}) for the shearing C mode[17] are not typically observed with commercial single-grating Raman instruments that operates in a backscattering geometry,[11] the two remaining modes, E^1_{2g} (384 cm^{-1}) and A_{1g} (408 cm^{-1}), have been routinely monitored for the diagnostic purpose. As decreasing the thickness, it was found that the peak frequency of A_{1g}, $\omega(A_{1g})$, gradually down-shifted, reaching 403 cm^{-1} for 1L.[11] The mode stiffening in A_{1g} with increasing thickness can be easily understood in analogy with two mechanical harmonic oscillators coupled by a weak spring which increases the overall restoring force, thus resulting in a resonance frequency higher than that of a single isolated oscillator.[11] However, the observation that E^1_{2g} softens with increasing thickness contrasted the simple mechanical model.[11] A recent theoretical work attributed this anomalous phonon dynamics to thickness-dependent dielectric constant which is larger for thicker MoS_2.[18] In essence, the ionic bonding between Mo and S atoms will be less screened in 1L MoS_2 than thicker ones, resulting in the anomalous frequency change. The Raman spectra obtained from pristine 1L-3L MoS_2 in Figure 2(a) nicely reproduced the findings of Lee *et al.*[11] The peak intensity of both Raman modes increased monotonically with increasing thickness. The frequency difference, $\Delta\omega = \omega(A_{1g}) - \omega(E^1_{2g})$, served as a spectroscopic indicator for the thickness as Lee *et al.* proposed.[11] For our pristine samples, $\Delta\omega$ was ~19.0, ~21.5 and ~23.5 cm^{-1} respectively for 1L, 2L and 3L, which agrees with the literature.[11]

The PL spectra of the pristine samples shown in Figure 2(b) were also consistent with the previous studies, confirming the high quality of the employed samples.[3] The prominent PL peaks denoted A (~1.84 eV) and B (~2.00 eV) originate respectively from the A and B excitons that are

split due to the spin-orbit coupling in the valence band.[3] It is also to be noted that the thickness-normalized PL intensity is the higher for the thinner layer. This apparent anomaly can be attributed to the indirect-to-direct bandgap transition when the number of layers reaches 1L.[3] Regarding this, Mak *et al.* showed that the PL quantum efficiency of freestanding 1L MoS_2 can be ~1000 times higher than that of bulk counterpart.[3] In order to investigate the possibility of thermally modulating the PL efficiency, 1L samples were annealed at elevated temperatures in a vacuum or high purity H_2 gas followed by the Raman and PL measurements. Figure 3(a) shows that the Raman spectra underwent negligible changes for either treatment except the slight peak frequency changes for the H_2-annealed 1L, which turned out to be sample-dependent. We speculate the changes are mainly due to thermally induced mechanical strain and charge doping as observed in graphene.[19] In contrast, the PL spectra in Figure 3(b) exhibited drastic changes for both cases. We first note that the vacuum-annealing increased the PL intensity (I_A) and peak energy (E_A) of A exciton by ~60% and ~20 meV, respectively. When annealed in H_2 gas, however, the opposite change was observed for the A exciton peak as shown by ~50% and ~20 meV decreases in I_A and E_A. It is to be noted that the PL signal attenuated by the H_2-treatment can be recovered by subsequent annealing in a vacuum (Fig. 3(b)), indicating that the change is reversible and thus unlikely due to structural defects in MoS_2. This result indicates that the electronic property of MoS_2 is greatly affected by the chemical nature of the ambient gas used in the thermal treatment.

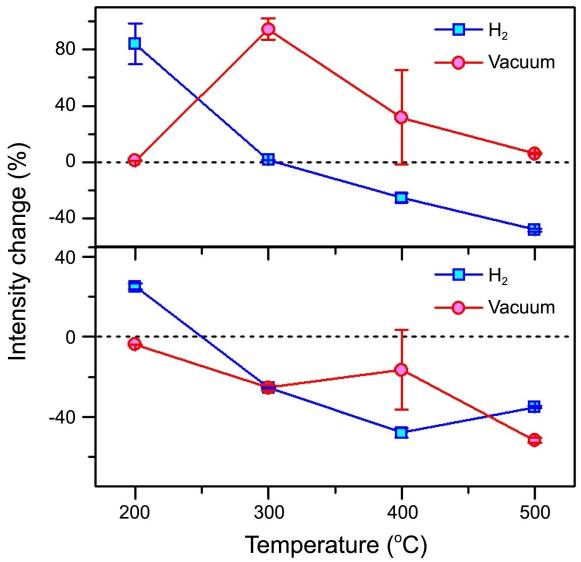

Figure 4. Thermally modulated PL intensities of 1L MoS_2. (Top) Relative change in I_A of annealed 1L samples with respect to their pristine state as a function of annealing temperature. (Bottom) Relative change in I_B of annealed 1L samples with respect to their pristine state. Circles and squares refer to samples annealed in a vacuum and H_2 gas, respectively. The error bars represent uncertainty originating from curve fittings using a double Lorentzian function except for the data of vacuum-annealing at 400 °C, which represents variation for multiple samples.

In Figure 4, we systematically investigated the thermally induced PL intensity changes for both A and B peaks. When annealed at 200 °C in a vacuum, there was no significant change in I_A. However, I_A increased by ~85% with respect to that of its pristine state when annealed at 300 °C. Further increase in the annealing temperature led to smaller enhancement, which finally returned back to zero for the annealing temperature of 500 °C. In contrast, the thermal treatment in H_2 gas induced a very different change in I_A. Whereas H_2-annealing at 200 °C resulted in ~80% increase in I_A, the PL intensity decreased as increasing the annealing temperature reaching 45% decrease at 500 °C. It should also be noted that E_A varied in opposite directions for the two different gas conditions as shown in Figure 3.

The observed PL change can be attributed to annealing-induced variation in charge density of 1L MoS_2. When electrical holes are injected into 1L MoS_2 and deplete the native n-type charge carriers,[8] I_A increases due to the attenuated nonradiative decay rate of the A exciton.[20] When electrons are introduced instead, enhanced nonradiative decay further decreases I_A.[20] Thus the significant rise in I_A for 300 °C suggests that the vacuum-annealing injects p-type charge carriers resulting in depletion of native n-type carriers, as proposed by Tongay *et al.*[20] The decrease in the enhancement at > 300 °C can be explained by the buildup of excess hole carriers that also promote the nonradiative decay of the A excitons.[20]

We note that annealing also induces p-type doping in graphene supported on silica substrates at > 200 °C and the degree of doping increases with increasing temperature of 600 °C.[21] A recent study[22] identified the ambient O_2 and water vapor as the dopants and proposed that they undergo an electrochemical redox reaction by borrowing electrons from graphene, which consequently becomes p-doped. It is also found that the molecular dopants are located between graphene and silica substrates,[23] suggesting the active role of hydrophilic silanol groups. Since the electrochemical potential for the redox couple[24] is lower than the Fermi level of MoS_2,[25] the electron transfer is thermodynamically favorable like the graphene system.[23] Thus, the observed p-doping induced by the vacuum-annealing is attributed to the following electrochemical reaction: $O_2 + 2H_2O + 4e^- \rightarrow 4OH^-$, where the electrons are transferred from MoS_2.

The overall PL attenuation caused by the H_2-treatment is attributed to n-type charge doping based on the PL energy change. The A peak consists of two sub-peaks, A^o and A^-, which originate from neutral excitons and negatively charged excitons, respectively.[8] Since the latter, also called trions, are formed when neutral excitons are combined through Coulomb attraction with excess electrons, E_{A^-} is ~20 meV smaller than E_{A^o}.[8] Thus A peak redshifts (blueshifts) and decreases (increases) in intensity due to the enhanced nonradiative decay when MoS_2 is doped with electrons (holes),[8] which agrees with the H_2-treated MoS_2 shown in Figure 3(b).

Currently, it is not clear how thermal treatment activates the proposed electrochemical reaction in MoS_2/SiO_2.[20] In

graphene/SiO_2 system, thermally induced nanoripples were suggested as active binding sites for the molecular p-type dopants.[22] However, Lee *et al.* showed that the thermal rippling occurs independently of the p-doping.[19] Inspired by a recent report that the dopants are located between graphene and SiO_2 substrates,[23] we propose that the thermal treatment modifies the surface functional groups of SiO_2 affecting the affinity for the dopants.[26] The presence of H_2 is likely to affect the chemical modification of SiO_2, leading to the observed sharp contrast in the PL spectra. The detailed mechanisms for the proposed changes are under systematic investigation and thus beyond the scope of the current report.

In summary, we reported that the PL spectrum of 1L MoS_2 was greatly affected by thermal annealing in a vacuum and the change was attributed to the p-type charge doping in MoS_2. The presence of H_2 gas lead to the opposite n-type doping, suggesting the possibility that the electronic properties can be tuned by a simple thermal treatment in a controlled gas environment.

Experimental

Single and few-layer MoS_2 were prepared by mechanically exfoliating 2H-MoS_2 crystals (SPI, molybdenite) onto a Si wafer substrate covered with a 285 nm thick amorphous SiO_2 layer.[11] Thin MoS_2 sheets of several μm across were identified under an optical microscope for faster screening and were probed with Raman spectroscopy for their thickness.[11] Raman and PL spectra were obtained with a home-built micro-Raman spectrometer setup that has been described in detail elsewhere.[27-29] Briefly, an Ar ion laser beam (514.5 nm, 0.17 mW) was focused onto a sample (spot size < 1 μm) using a microscope objective (40X, numerical aperture = 0.60). Back-scattered Raman or PL signal was collected with the same objective and guided to a spectrometer combined with a liquid nitrogen-cooled CCD detector. The overall spectral accuracy was better than 1 cm^{-1} and 1.5 meV for Raman and PL spectra, respectively. Atomic force microscopy (AFM) was also employed to reveal the nanoscopic morphology of the samples. To modify the PL characteristics, some samples were annealed in a vacuum (< 3 mtorr) or H_2 gas (99.999%, flow rate = 30 mL/min) using a tube furnace. The annealing time was one hour unless stated otherwise.

Acknowledgments. This work was supported by a grant from Kyung Hee University in 2010 (KHU-20101828).

References

1. Novoselov, K. S.; Geim, A. K.; Morozov, S. V.; Jiang, D.; Zhang, Y.; Dubonos, S. V.; Grigorieva, I. V.; Firsov, A. A. *Science* **2004**, *306*, 666.
2. Geim, A. K.; Novoselov, K. S. *Nat. Mater.* **2007**, *6*, 183.
3. Mak, K. F.; Lee, C.; Hone, J.; Shan, J.; Heinz, T. F. *Phys. Rev. Lett.* **2010**, *105*, 136805.
4. Dean, C. R.; Young, A. F.; Meric, I.; Lee, C.; Wang, L.; Sorgenfrei, S.; Watanabe, K.; Taniguchi, T.; Kim, P.; Shepard, K. L.; Hone, J. *Nat. Nanotechnol.* **2010**, *5*, 722.
5. Castro Neto, A. H.; Guinea, F.; Peres, N. M. R.; Novoselov, K. S.; Geim, A. K. *Rev. Mod. Phys.* **2009**, *81*, 109.
6. Splendiani, A.; Sun, L.; Zhang, Y. B.; Li, T. S.; Kim, J.; Chim, C. Y.; Galli, G.; Wang, F. *Nano Lett.* **2010**, *10*, 1271.
7. Mak, K. F.; He, K. L.; Shan, J.; Heinz, T. F. *Nat. Nanotechnol.* **2012**, *7*, 494.
8. Mak, K. F.; He, K.; Lee, C.; Lee, G. H.; Hone, J.; Heinz, T. F.; Shan, J. *Nat. Mater.* **2013**, *12*, 207.
9. Verble, J. L.; Wieting, T. J. *Phys. Rev. Lett.* **1970**, *25*, 362.
10. Mattheiss, L. F. *Phys. Rev. B* **1973**, *8*, 3719.
11. Lee, C.; Yan, H.; Brus, L. E.; Heinz, T. F.; Hone, J.; Ryu, S. *ACS Nano* **2010**, *4*, 2695.
12. Newaz, A. K. M.; Prasai, D.; Ziegler, J. I.; Caudel, D.; Robinson, S.; Haglund, R. F.; Bolotin, K. I. *Solid State Commun.* **2013**, *155*, 49.
13. Mak, K. F.; Sfeir, M. Y.; Misewich, J. A.; Heinz, T. F. *Proc. Natl. Acad. Sci. USA* **2010**, *107*, 14999.
14. Wakabayashi, N.; Smith, H. G.; Nicklow, R. M. *Phys. Rev. B* **1975**, *12*, 659.
15. Ferrari, A. C.; Basko, D. M. *Nat. Nanotechnol.* **2013**, *8*, 235.
16. Ferrari, A. C. *Solid State Commun.* **2007**, *143*, 47.
17. Zhang, X.; Han, W. P.; Wu, J. B.; Milana, S.; Lu, Y.; Li, Q. Q.; Ferrari, A. C.; Tan, P. H. *Phys. Rev. B* **2013**, *87*, 115413.
18. Molina-Sanchez, A.; Wirtz, L. *Phys. Rev. B* **2011**, *84*, 155413.
19. Lee, J. E.; Ahn, G.; Shim, J.; Lee, Y. S.; Ryu, S. *Nat. Commun.* **2012**, *3*, 1024.
20. Tongay, S.; Zhou, J.; Ataca, C.; Liu, J.; Kang, J. S.; Matthews, T. S.; You, L.; Li, J.; Grossman, J. C.; Wu, J. *Nano Lett.* **2013**, *13*, 2831.
21. Liu, L.; Ryu, S.; Tomasik, M. R.; Stolyarova, E.; Jung, N.; Hybertsen, M. S.; Steigerwald, M. L.; Brus, L. E.; Flynn, G. W. *Nano Lett.* **2008**, *8*, 1965.
22. Ryu, S.; Liu, L.; Berciaud, S.; Yu, Y.-J.; Liu, H.; Kim, P.; Flynn, G. W.; Brus, L. E. *Nano Lett.* **2010**, *10*, 4944.
23. Lee, D.; Ahn, G.; Ryu, S. **2014**, submitted.
24. Chakrapani, V.; Angus, J. C.; Anderson, A. B.; Wolter, S. D.; Stoner, B. R.; Sumanasekera, G. U. *Science* **2007**, *318*, 1424.
25. Fontana, M.; Deppe, T.; Boyd, A. K.; Rinzan, M.; Liu, A. Y.; Paranjape, M.; Barbara, P. *Sci. Rep.* **2013**, *3*, 1634.
26. Zhuravlev, L. T. *Colloids Surf. A* **2000**, *173*, 1.
27. Ahn, G.; Kim, H. R.; Ko, T. Y.; Choi, K.; Watanabe, K.; Taniguchi, T.; Hong, B. H.; Ryu, S. *ACS Nano* **2013**, *7*, 1533.
28. Shim, J.; Lui, C. H.; Ko, T. Y.; Yu, Y.-J.; Kim, P.; Heinz, T. F.; Ryu, S. *Nano Lett.* **2012**, *12*, 648.
29. Ryu, S.; Maultzsch, J.; Han, M. Y.; Kim, P.; Brus, L. E. *ACS Nano* **2011**, *5*, 4123.